Aalborg Universitet

Static Tension Tests on Axially Loaded Pile Segments in Sand

Thomassen, Kristina; Andersen, Lars Vabbersgaard; Ibsen, Lars Bo

[Link to publication from Aalborg University](#)

Static Tension Tests on Axially Loaded Pile Segments in Sand

Kristina Thomassen

Lars Vabbersgaard Andersen

Lars Bo Ibsen

Aalborg University

Department of Civil Engineering

Division for Structures, Materials and Geotechnics

DCE Technical Report No. 206

March 2016

Scientific Publications at the Department of Civil Engineering

Technical Reports are published for timely dissemination of research results and scientific work carried out at the Department of Civil Engineering (DCE) at Aalborg University. This medium allows publication of more detailed explanations and results than typically allowed in scientific journals.

Technical Memoranda are produced to enable the preliminary dissemination of scientific work by the personnel of the DCE where such release is deemed to be appropriate. Documents of this kind may be incomplete or temporary versions of papers—or part of continuing work. This should be kept in mind when references are given to publications of this kind.

Contract Reports are produced to report scientific work carried out under contract. Publications of this kind contain confidential matter and are reserved for the sponsors and the DCE. Therefore, Contract Reports are generally not available for public circulation.

Lecture Notes contain material produced by the lecturers at the DCE for educational purposes. This may be scientific notes, lecture books, example problems or manuals for laboratory work, or computer programs developed at the DCE.

Theses are monograms or collections of papers published to report the scientific work carried out at the DCE to obtain a degree as either PhD or Doctor of Technology. The thesis is publicly available after the defence of the degree.

Latest News is published to enable rapid communication of information about scientific work carried out at the DCE. This includes the status of research projects, developments in the laboratories, information about collaborative work and recent research results.

ABSTRACT

This paper provides laboratory test results of static axially loaded piles in sand. With a newly developed test setup, the pile-soil interface friction was investigated by using an open-ended steel pile segment with a diameter of 0.5 m. Use of a pile length of 1 m enabled the pile-soil interface friction to be analyzed at a given soil horizon while increasing the vertical effective stress in the sand. Test results obtained by this approach can be analyzed as single *t-z* curves and compared to predictions of unit shaft friction from current design methods for offshore foundations. The test results showed best agreement with the traditional design method given in the American Petroleum Institute (API) design code. When *t-z* curves obtained from the test results were compared to *t-z* curve formulations found in the literature, the Zhang formulation gave good predictions of the initial and post-peak parts of the *t-z* curves found in the test results.

1. INTRODUCTION

When the water depth exceeds 30 m, a jacket foundation with three or four legs becomes appropriate as the foundation for offshore wind turbines. Due to the light weight of wind turbine structures, one or more of these piles are sometimes loaded in tension. This situation has not been well examined because the primary use of pile foundations offshore has been in the oil and gas industry. In these applications, the weight of the structures is high compared to the horizontal loads from wind and waves, resulting in piles loaded in compression. Thus, research is needed within the field of axially loaded piles in tension.

Due to the expense, few full-scale tests have been conducted on offshore piles (e.g., Jardine and Standing 2012; Baeβler et al. 2013). Instead, pile behavior has been examined on the small scale in calibration chambers (e.g., Chan and Hanna 1980; Jardine et al. 2009; Le Kouby et al. 2004) by using closed-ended piles of stainless steel or aluminum. The pile roughness was reduced to minimize scaling effects due to the relatively small size of the sand grains compared to the diameter of the pile.

The present research analyzed the resistance against pull-out of an axially loaded pile in dense to very dense sand, resembling the soil conditions found at specific wind park locations in the North Sea. The test setup attempted to model the pile-soil interface friction accurately, by using an open-ended steel pile segment with a diameter of 0.5 m, which is close to the diameter of the full-scale pile. Use of a pile length of 1 m enabled the pile-soil interface friction to be analyzed at a given soil horizon while increasing the effective stress in the sand. Hence, *t-z* curves for different vertical effective stress levels could be determined and analyzed. The aim of the research was to determine the pull-out resistance of a pile in the serviceability mode (i.e., when the effect of the installation on the bearing capacity is reduced because of setup over time). Instead of installing the pile and leaving it in the test setup for a period of time before testing, the sand was processed after pile installation to a state thought to resemble the serviceability mode

Short descriptions of the test setup and test procedure are given, followed by the test results in the form of the measured bearing capacity of the pile segment. The results are compared to the unit skin friction determined from current design methods. Moreover, *t-z* curves are obtained from the test results and compared to expressions from the literature.
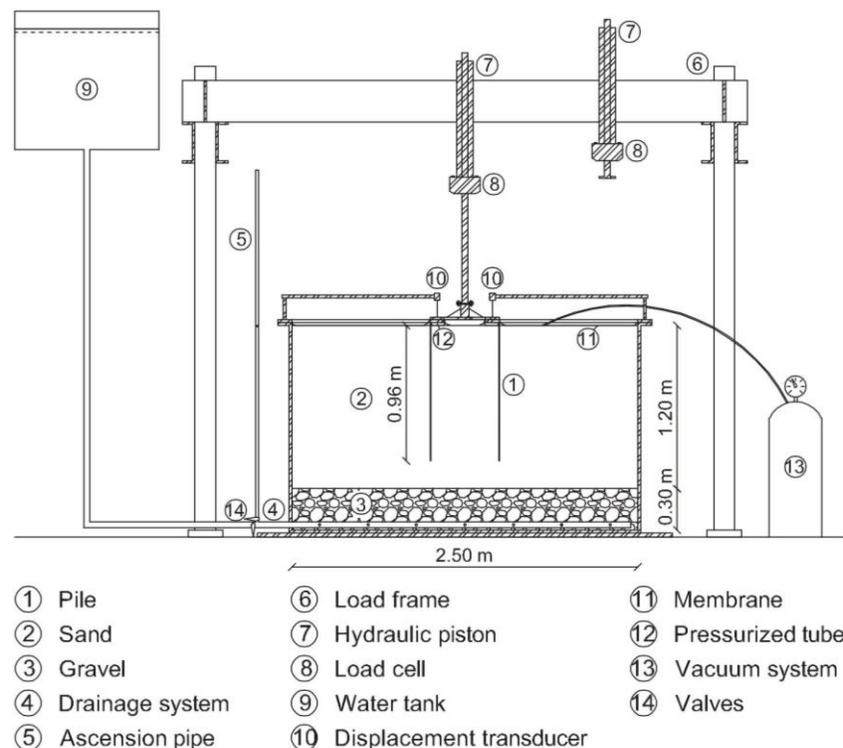
2. METHODOLOGY AND TEST PROGRAM

2.1. Test Setup

Figs. 1 and 2 show the test setup that consisted of a box of 2.5 m in diameter with a layer of dense sand of 1.2 m in depth. The hydraulic cylinder on the right was used to install the pile segment and to conduct cone penetration tests (CPTs). The hydraulic cylinder on the left was used during tests. The test sand was Aalborg University Sand No. 1 with the material properties given in Table 1. Comprehensive descriptions of the test setup and sand processing procedure are provided by Thomassen et al. ("Laboratory Test Setup for Cyclic Axially Loaded Piles in Sand," submitted, Aalborg University, Denmark).

Table 1. Material Properties of Aalborg University Sand No. 1 (Hedegaard and Borup 1993)

d_s (g/cm^3)	e_{max} (-)	e_{min} (-)	d_{50} (mm)	$c_u = d_{60}/d_{10}$ (-)
2.64	0.854	0.549	0.14	1.78

① Pile	⑥ Load frame	⑪ Membrane
② Sand	⑦ Hydraulic piston	⑫ Pressurized tube
③ Gravel	⑧ Load cell	⑬ Vacuum system
④ Drainage system	⑨ Water tank	⑭ Valves
⑤ Ascension pipe	⑩ Displacement transducer	

Fig. 1. Schematic illustration of the test setup.

Fig. 2. Setup for a test with applied suction.

The pile segment used in the tests had an outer diameter of $D = 0.5$ m, pile wall thickness of $t = 0.003$ m, and embedded length of $L_p = 0.96$ m. The segment was made of steel, which resulted in a corroded pile surface to obtain the correct pile-soil interface properties. To minimize any contribution from base resistance in the planned cyclic loading tests, the wall thickness was chosen to be as small as possible without risking instability problems during pile installation. The idea of using a pile with a length of 0.96 m was to enable laboratory tests on a large-diameter pile, while increasing the vertical effective stress in the soil to simulate pile segments at different soil depths. The vertical effective stress in the soil was increased by using a membrane-vacuum system. An elastic rubber membrane was placed on the soil surface and tightened at the sandbox edge to create an airtight system coupled to a vacuum pump. The vertical effective stress was increased by applying suction to the sandbox through five quick couplings placed on the membrane.

2.2. Test Procedure

Sand in the sandbox was not replaced between tests. Instead, it was loosened by a hydraulic gradient, $i = 0.9 i_{crit}$, to rehomogenize the soil after the previous test. The pile segment was then installed in the sand, which was then prepared to the desired relative density by a rod vibrator. The relative density of sand before the tests was approximately 85%. During a test, sand very close to the interface was affected by shearing, which might lead to grain crushing. The soil loosening and vibrating steps were assumed to rearrange the grains, resulting in new and undamaged interface conditions for each test. Thus, the bearing capacity of the pile segment was not influenced by any installation mechanism.

9

Seven static tension tests were conducted at suction levels of 0, 20, 35, and 70 kPa. These displacement-controlled tests were conducted at a displacement rate of 0.002 mm/s. During the tests, the pile head displacement, resulting load, and suction level were measured.

2.3. Expected Results

Test results are affected by the conditions of the test setup and test specimen, such as the pile-soil interface properties, installation method, pile segment dimensions, and boundary conditions. Effects of these parameters have been examined for different test setups in the literature. Interface conditions are affected by the relative density of the sand, relative interface roughness, sand grain properties (e.g., shape and size), and normal stress on the interface. Shear box tests under conditions of constant normal load and constant normal stiffness have revealed that, in the case of dense sand and high relative interface roughness, dilation occurs within the first few millimeters of displacement, with a subsequent decrease to a residual value of interface shear strength (Prai-ai 2013; Mortara 2007; Hammad 1991; Boulon 1989; Uesugi and Kishida 1986). Dilatant behavior at the pile-soil interface induces a radial stress change that is dependent on the pile diameter (Boulon and Foray 1986) and may be significant for piles with $D < 1$ m (Jardine et al., 2005). Angular sand grains lead to a higher interface shear strength compared to rounded sand grains. Increased normal stresses on the interface will increase the interface shear strength. A virgin pile-soil interface, with sand prepared around the test pile, may show a peak followed by a decrease in shaft friction due to sand grain rearrangements during loading (Le Kouby et al. 2013). During pile installation, the grains are rearranged and likely crushed, which may affect the load-displacement curve such that no peak load occurs (Le Kouby et al. 2013).

The effect of the lateral boundary conditions has mostly been examined by penetration tests (Huang and Hsu 2005; Salgado et al. 1998; Schnaid and Houlsby 1991; Foray 1991; Ghionna and Jamiolkowski 1991). In a calibration chamber with rigid lateral boundaries, no lateral displacement occurs at the boundaries. When sand at the boundary is affected by pile loading, the pull-out resistance might be higher than the results of similar tests in free field (Salgado et al. 1998).

The above-mentioned effects on pile test results lead to some expected effects for the present study. For example, an increase of the vertical effective stress in the sand would lead to increases in the horizontal stress and the pull-out capacity of the pile segment. Dilation was expected because of the high relative density of the sand and high relative interface roughness. Moreover, the pile-soil interface was thought to have properties comparable to those of a virgin interface, due to the soil processing procedure. As a result, the shaft friction may peak and subsequently decline. Finally, due to the rigid lateral boundaries, higher capacities may be found in the present tests compared to tests conducted in free field.

3. TEST RESULTS

The following sections present the load-displacement curves obtained in the tests, as well as observations made during and after the tests. Tension load and resulting upward

displacements of the pile are defined as negative. As suction is assumed to increase the effective stress to the same extent as an applied overburden pressure, the applied suction is defined as positive. Test results are compared to results obtained in a Plaxis model of the test setup.

3.1. Recorded Load-Displacement Curves

Fig. 3 displays the load-displacement curves for all tests. All curves show the expected peak load. However, peaks of curves for tests at suction levels (surcharges) of 35 and 70 kPa are much more distinct than peaks at 0 and 20 kPa. Partial plugging was observed in all tests because the surface inside the pile was elevated approximately 30 mm compared to the outside sand surface.

In tests with the membrane, the water was not de-aired before the tests, and the setup was not 100% hermetically sealed. This meant that most of the water was sucked out of the system before the test. Thus, sand was only partly saturated during tests with the membrane and applied suction (Fig. 4). In these tests, sand near the pile-soil interface was stuck to the piles. In tests without applied suction, the sand was saturated throughout the test and did not stick to the pile during pull-out.

Fig. 5 shows the uninstallation of the pile after a test with applied suction. The sand was not saturated before uninstallation and remained stuck to the upper one third of the pile shaft when the pile was pulled out of the sand. These observations implied that part of the failure happened in the sand and not at the pile-soil interface. This fact may have an increasing effect on the difference between the peak and residual values of the measured force during the tests, because a sand-sand shear band experiences greater dilation than a soil-plate interface (Lehane et al. 1993). Another explanation of the distinct peaks may be that part of the soil plug stopped moving along with the pile at some point during the tests.
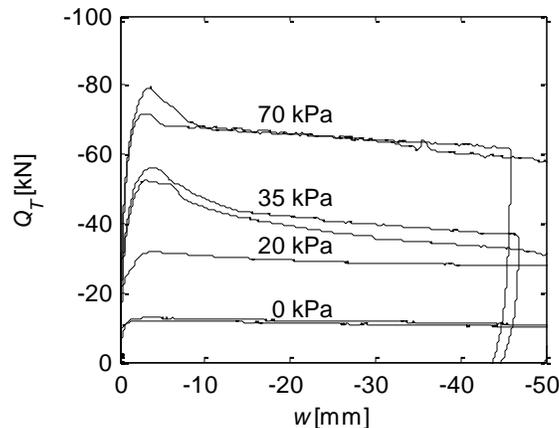

Fig. 3. Measured pull-out force versus pile head displacement. Surcharge is indicated in each test.

Fig. 4. After tests with applied suction, sand in the interface is stuck to the pile.

Fig. 5. Uninstallation of the pile after a test with applied suction. Sand is not resaturated before uninstallation, and some sand is stuck to the upper one third of the pile.

3.2. Comparison to Finite Element Models

Tests at 0, 35, and 70 kPa were modelled as axisymmetric models in PLAXIS 2D AE to get a better understanding of the test mechanisms. To model the change in vertical effective stress obtained by applying suction to the sandbox, a surface load, P_0, of the same magnitude was applied in the PLAXIS models. In these models, the sand was considered unsaturated. In the model without overburden pressure, the sand was saturated.

Table 2 shows the material properties, which were chosen to resemble the conditions in the real test setup. Friction and dilation angles were determined from the results of CPTs conducted before each test by the method described in Ibsen et al. (2009). The

constant volume interface friction angle, δ_{cv}, was chosen to be 28.8°. Ho et al. (2011) suggested a dependency of δ_{cv} on d_{50} and the interface displacement. For d_{50} = 0.14 (Aalborg University Sand No. 1), δ_{cv} is very close to the value of 28.8° recommended for CPT-based methods (Jardine et al. 2005; API 2011; Jardine et al. 1992). Table 3 gives the material properties of the pile, which are the same as for the pile segment used in the test setup.

To obtain force values that were similar to the residual values of forces measured in the physical tests, high values of the coefficient of lateral earth pressure at rest, K_0, had to be used in the models (i.e., K_0 = 3 for P_0 = 0 or 35 kPa, and K_0 = 5 for P_0 = 70 kPa). Fig. 6 shows the comparison between the test results and the Plaxis calculations. The large values of K_0 may be reasonable, as flat dilatometer tests conducted in the sandbox by Gaydadzhiev et al. (2015) showed that K_0 values vary between 0.5 and 5. Soil processing with the rod vibrator may have introduced a large degree of overconsolidation. To reach the peak values from the tests in the PLAXIS models, either much higher values of K_0 or higher interface friction values must be applied.
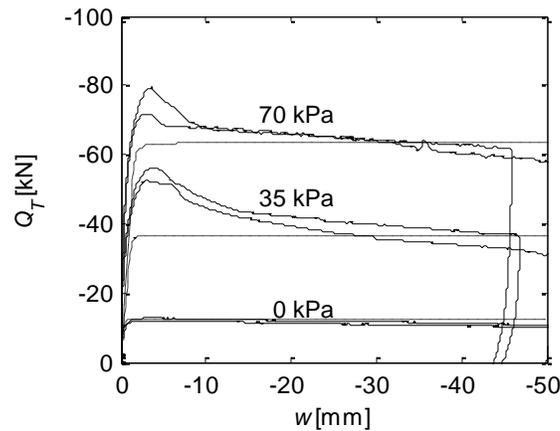

Fig. 6. Plaxis results versus test results. Dashed lines are Plaxis results with K_0 = 3 for surcharges of 0 and 35 kPa, and with K_0 = 5 for a surcharge of 70 kPa.

Table 2. Material Properties of the Sand and Interfaces.

Parameter	Unit	Sand (0 kPa)	Sand (35 kPa)	Sand (70 kPa)	Gravel
General					
Material model	-	MC	MC	MC	MC
Type of material behavior	-	Drained	Drained	Drained	Drained
Soil unit weight above phreatic level, γ_{unsat}	kN/m^3	17	17	17	18
Soil unit weight below phreatic level, γ_{sat}	kN/m^3	20	20	20	20
Parameters					
Young's modulus, E'	kN/m^2	13400	17000	23600	45000
Poisson's ratio, v'	-	0.23	0.23	0.23	0.3
Cohesion (constant), c'_{ref}	kN/m^2	0.1	0.1	0.1	0.1
Friction angle, φ'	°	53.0	51.0	48.1	45
Dilation angle, ψ	°	19.0	18.7	17.8	15
Interface friction angle, δ_{cv}	°	28.8	28.8	28.8	-
R_{inter} ($\tan\delta_{cv} / \tan\varphi'$)	-	0.41	0.45	0.49	-

Table 3. Material Properties of the Pile (Shell).

Parameter	Unit	Pile
Material type	-	Elastic, isotropic
Axial stiffness, EA	kN/m	630000
Flexural rigidity, EI	kN·m^2/m	0.4725
Specific weight, w	kN/m/m	0.52
Poisson's ratio, v	-	0.3

Even if the residual force was obtained in the PLAXIS models, the displacement of the soil plug was smaller than the displacement observed in the tests. However, during the first part of the loading in PLAXIS, the soil moved up along with the pile (although soil may not have moved at the same rate as the pile). As loading continued, the bottom part of the soil plug stopped moving. This implies that the force measured in the laboratory tests included the weight of the entire soil plug at the beginning of the test. As the test proceeded, this weight was reduced to around two thirds of the total soil plug

14

weight. These observations may explain the observed large peak force. Of course, the explanation implies that an internal friction along the pile shaft was not activated when the soil plug stopped moving.

3.3. Shaft Friction

Due to partial plugging, it was difficult to determine the contribution of the internal skin friction on the pile segment wall to the skin friction resistance, Q_s. The contribution can be assumed to range between no contribution (fully plugged) and complete contribution (unplugged). This relationship can be expressed as follows:

$$Q_{s,plugged} = Q_T - W_{pile} - W_{plug} \tag{1}$$

$$Q_{s,unplugged} = Q_T - W_{pile} \tag{2}$$

where W_{pile} is the weight of the pile segment and equipment under the load cell, and W_{plug} is the weight of the soil plug.

Fig. 7 shows the difference between Eqs. 1 and 2, using a test conducted at 70 kPa as an example. However, even the situation of a fully plugged pile during the first millimeters of displacement and a fully unplugged pile for the remainder of the test does not explain the distinct peak of the load-displacement curve. Therefore, the skin friction resistance, Q_s, is given as

$$Q_s = A_s \int_0^{L_P} f_s dz \tag{3}$$

where A_s is the pile area per unit length of the pile, L_p is the pile tip depth, and f_s is the unit shaft friction at depth z. For the plugged case, A_s is the external pile area. For the unplugged case, A_s is both the internal and external pile area. Fig. 8 displays the unit shaft friction for these two conditions, for a test conducted at 70 kPa.

In the next section, the unit skin friction obtained from the test results is compared to the results from current design methods. Moreover, t-z curves are derived from the test results and compared to expressions for t-z curves given in the literature.
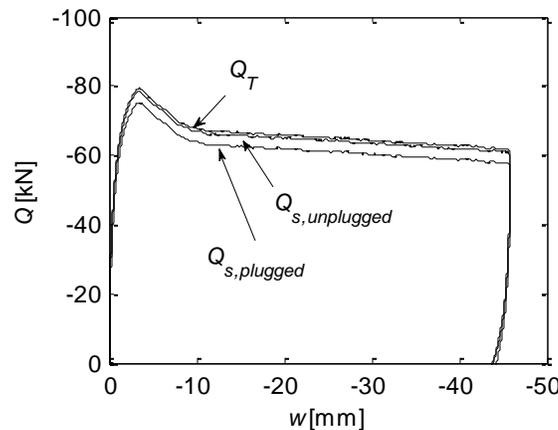

Fig. 7. Difference between fully plugged and unplugged determinations of Q_s for a test conducted
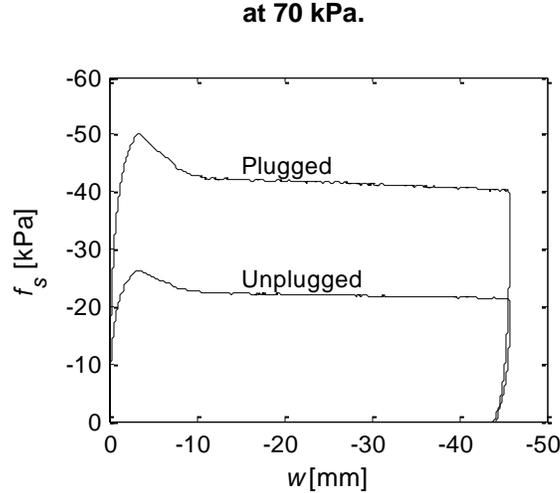
at 70 kPa.

Fig. 8. Unit shaft friction versus pile head displacement for the plugged and unplugged cases, for a test conducted at 70 kPa.

4. COMPARISON TO EXISTING DESIGN METHODS

The test results were compared to the traditional design methods given by the American Petroleum Institute (API) (API 2011) and to CPT-based design methods. The desired outcome was a formulation of f_s expressed as an empirical coefficient, k_f, relating the average cone resistance, q_c, at depth z to the skin friction, f_s, such as:

$$f_s = k_f q_c \tag{4}$$

k_f factors were found for the design methods and compared to those of the test results.
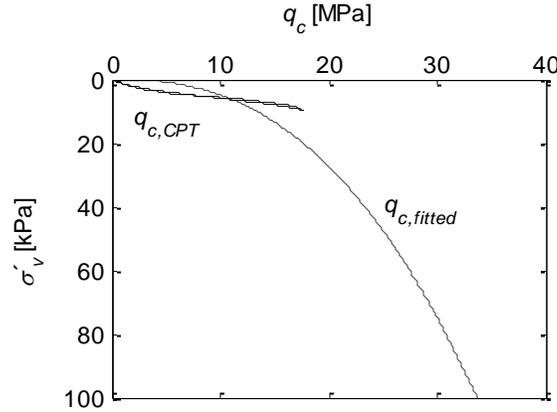
4.1. CPT Cone Resistance

To find the k_f factors, the CPT cone resistance in the sandbox had to be known. Before each test, CPTs were performed to determine the relative density of the sand. CPT results could only be used for tests without applied suction; a CPT could not be conducted when the pile segment was installed and a membrane was placed on the sand surface. Therefore, no q_c measurements relating directly to each test were available. However, Gaydadzhiev et al. (2015) conducted CPTs in the sandbox at different stress levels without any test specimens installed.

The empirical relationship between the effective vertical stress, σ'_v, and the CPT cone resistance, q_c, had the form:

$$q_{c,fitted} = 5324.1 kPa \left(\frac{\sigma'_v}{1kPa}\right)^{0.3998}. \tag{5}$$

Fig. 9 shows q_c as a function of σ'_v based on Eq. 5 and the q_c values from CPTs conducted before tests without applied suction. Although the q_c profiles are different, the $\int q_c$ results from tests without applied suction do not differ substantially. Thus, results from the fitted profile were used in the comparison of all tests. For tests without applied suction, σ'_v was calculated by assuming that the sand was saturated throughout the test. For tests with a membrane and applied suction, σ'_v was calculated by assuming

16

unsaturated sand, because most of the water was sucked out of the sandbox before the test.

Fig. 9. Cone resistance based on CPTs conducted before tests without suction and on the fitted expression given by Eq. 5 versus the vertical effective stress.

4.2. Traditional Design Method

The API (2011) suggests the following definition of the unit shaft friction:

$$f_s = \beta \sigma'_v = K_f \tan(\delta)\sigma'_v \tag{6}$$

where β is a dimensionless shaft friction factor, σ'_v is the effective vertical stress at a given depth, K is the coefficient of lateral earth pressure, and δ is the interface friction angle. As K was unknown, the recommendations given in API (2011) for $D_r = 0.85$ were followed; hence, $\beta = 0.56$.

4.3. CPT-based Methods

The Det norske Veritas (DNV) (DNV 1992) proposed the simplest form of a CPT-based method, in which k_f is given in terms of a most probable value (0.001) and a highest expected value (0.003). More advanced CPT-based methods include the ICP-05, UWA-05, and NGI-05 methods, which all account for the stress state, pile dimensions and material, as well as installation effects (Jardine et al. 2005; Lehane et al. 2005b; Clausen et al. 2005).

The ICP-05 and UWA-05 methods follow the Coulomb criterion,

$$f_s = \sigma'_{rf} \tan \delta_{cv} = (\sigma'_{rc} + \Delta\sigma'_{rd}) \tan \delta_{cv} \tag{7}$$

where σ'_{rf} is the radial effective stress at failure, δ_{cv} is the constant volume interface friction angle, σ'_{rc} is the radial effective stress after installation and equalization, and $\Delta\sigma'_{rd}$ is the change in radial stress due to the loading stress path (dilation). Expressions for σ'_{rc} and $\Delta\sigma'_{rd}$ vary for the ICP-05 and UWA-05 methods. The contribution from dilation may be important for piles with a diameter less than 1 m, whereas the contribution is negligible for full-scale offshore piles (Jardine et al. 2005).

For offshore piles, the API (2011) suggests a simplified expression of the ICP-05 and

UWA-05 methods for f_s, given by

$$f_s = u \left(\frac{\sigma_v'}{p_a}\right)^a A_r^b \max\left(\frac{h}{D}, v\right)^{-c} \tan(\delta_{cv}) \, q_c \tag{8}$$

where σ_v' is the local vertical effective stress; p_a is a reference stress (100 kPa); $A_r = 1 - (D_i/D)^2$ is the effective area ratio; h is the distance above the pile tip; D and D_i are the outer and inner pile diameters, respectively; δ_{cv} is the interface friction angle; q_c is the local cone resistance; and u, a, b, c, and v are constants with the values given in Table 4. Eq. 8 assumes a negligible contribution from dilation, and assumes that the piles are open-ended pipe piles driven unplugged but failing plugged. This expression was used in the following analyses.

Table 4. Unit Shaft Friction Values for Open-Ended Steel Piles Loaded in Tension (API 2011).

Method	a	b	c	u	v
Simplified ICP	0.1	0.2	0.4	0.016	$4\sqrt{A_r}$
Offshore UWA	0.0	0.3	0.5	0.022	2

Eq. 8 contains installation effects that were absent from the test results due to the use of the soil preparation procedure. First, the effective area ratio, A_r, accounts for changes in radial stress at the pile tip during installation. This ratio is related to the amount of soil that is displaced during installation and depends on whether the pile is closed-ended ($A_r = 1$), partially plugged ($0.1 < A_r < 1$), or unplugged ($A_r = 0.1$). The very small wall thickness of the test specimen (3 mm) resulted in a factor of 0.0239, which was lower than the unplugged value of $A_r = 0.1$ and indicated a very low disturbance of the soil during installation. As it was assumed that there were no installation effects, this term was included when comparing the test results to the design methods. Second, h/D is the friction fatigue effect that is related to installation. At a given soil horizon, the radial stress decreases as the pile tip moves further into the soil. h/D was ignored in the comparison of the test results, leaving a simplified expression for k_f:

$$k_f = u \left(\frac{\sigma_v'}{p_a}\right)^a A_r^b \tan(\delta_{cv}) \tag{9}$$

Fig. 10 shows the k_f factors calculated based on the test results, the API method, and the CPT-based methods. The k_f factors for the test results were based on the maximum values of f_s for the plugged calculation. For the unplugged calculation, the k_f factors would decrease by nearly one half. The test results suggested a stress dependency of k_f, which resulted in an expression based on Eq. 9 with the factor $u = 0.01$ and powers $a = b = 0.3$.

The k_f factors determined by the API method are very different from the ones determined by the simplified ICP and offshore UWA methods. This observation is in agreement with the conclusions of the database study performed by Lehane et al. (2005a), in which the API method seemed to underpredict the capacity of short piles in dense sand. However, for the current test results, the API method gave the best prediction of the unit shaft friction.
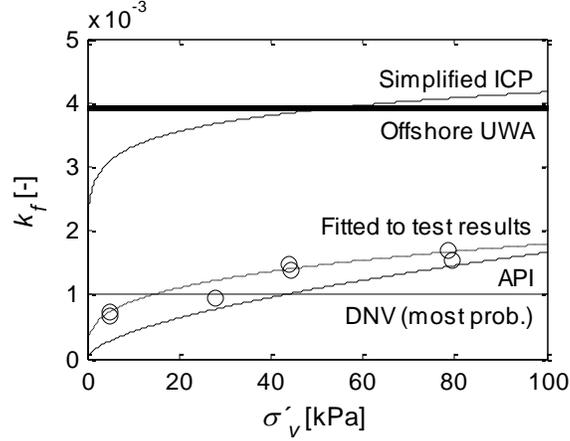
Fig. 10. k_f factors calculated based on the test results, the API method, and the CPT-based methods.

In the analysis of the k_f factors, the effects of dilation on the radial effective stress of the pile were not taken into account because the unit skin friction in the simplified ICP-05 and UWA-05 methods has a simpler formulation where the dilation term is excluded. However, because the pile segment used in the tests had a diameter of 0.5 m (i.e., < 1 m), the contribution of dilation-induced changes in the radial effective stress must be examined. The change in radial stress due to dilation is given by (Jardine et al. 2005; Lehane et al. 2005b):

$$\Delta\sigma'_{rd} = 4G \frac{\Delta r}{D} \tag{10}$$

where G is the shear modulus of sand, and Δr is the radial displacement in the interface shear zone (assumed to be 0.02 mm for a lightly rusted pile). The UWA-05 and ICP-05 methods calculate the shear modulus differently, although both expressions are based on Baldi et al. (1986). The UWA-05 method suggests the following expression for the shear modulus:

$$G_{UWA} = 185 q_c q_{cN1}^{-0.7} \tag{11}$$

$$q_{cN1} = \frac{q_c/p_a}{(\sigma'_{v0}/p_a)^{0.5}} \tag{12}$$

The ICP-05 method gives the following definition:

$$G_{ICP} = G_0 = q_c(0.0203 + 0.00125\eta - 1.21 \cdot 10^{-5}\eta^2)^{-1} \tag{13}$$

$$\eta = \frac{q_c}{(\sigma'_{v0} p_a)^{0.5}} \tag{14}$$

where q_c is the average cone resistance at depth z, p_a is the reference stress (100 kPa), and σ'_{v0} is the effective vertical stress at a given depth.

When dilation effects were included in the calculation of f_s based on the UWA-05 method, the contribution was negligible (approximately 4%). However, for the ICP-05 method, the contribution lay between 7% and 10%, increasing with decreasing effective vertical stress, and should be taken into account. If the contribution is compared directly to the test results, then the UWA method predicts that 10–30% of the unit skin friction

19

stems from dilation effects, which increases with decreasing vertical effective stress. The ICP method predicts contributions of 16–45%. These contributions are substantial; thus, the proposed expression of the k_f factor for the test results should include a term accounting for the dilation effects.

5. t-z CURVES

Various t-z curve formulations are used to determine the pile-shaft response of axially loaded piles. Some of these formulations are used in this paper in the comparison to the t-z curves obtained from the test results (see Appendix A). API (2011) gives the simplest of these formulations. More advanced formulations include the parabolic function (Randolph and Gourvenec 2011), 80% function (Fellenius 2013), and Zhang function (Zhang and Zhang 2012) that all introduce nonlinear variations in the initial parts of the curves and the possibility of modelling strain-softening.

To compare the methods to the t-z curves obtained from the test results, an average displacement corresponding to the maximum unit skin friction ($z_{tmax} = 3.5$ mm) and an average ratio between the residual and maximum unit skin frictions ($\beta_s = t_{res}/t_{max} = 0.81$) were used. The method gave good estimates for most of the test results, except for the two tests conducted with a surcharge of 35 kPa (Fig 11). For these two tests, however, the 80% function was in good agreement with the strain-softening behavior observed in the tests.

Fig. 12 shows the initial part of the t-z curves. The 80% function and the Zhang function provided the best agreement with the initial part of the test results, whereas the API formulation gave poor predictions of the initial and post-peak parts of the test t-z curves. Of the four presented formulations, the Zhang function had the best fit to the test t-z curves.
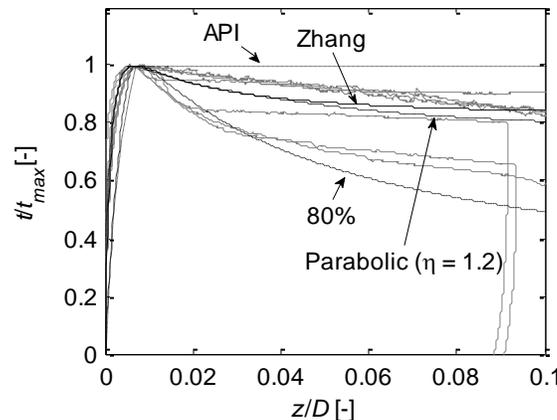

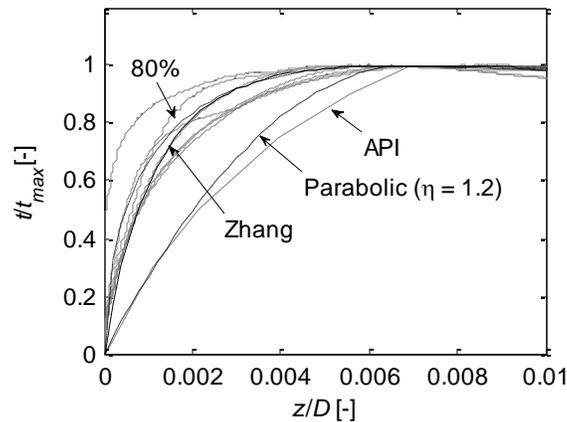**Fig. 11. Various t-z curves compared to the t-z curves obtained from the test results (gray).**

Fig. 12. Initial part of the *t-z* curves displayed by Fig. 11.

6. CONCLUSION

This paper presented seven static axial loading tests on a pile segment installed in dense sand in a laboratory setup. To model the pile-soil interface properties to be as close as possible to the properties of full-scale piles, a pile segment diameter of 0.5 m was chosen. To accommodate this diameter in the test setup, the pile segment was 0.96 m long, and the vertical effective stresses in the soil were increased by a vacuum system. Thus, each test simulated a segment of a pile at different overburden pressures. By comparing the test results to PLAXIS models of each test, it was concluded that the sand was highly overconsolidated due to the soil preparation procedure in order to produce the determined pull-out capacities.

The unit shaft friction was found from the test results by determining the k_f factor linking the CPT cone resistance in the sand to the unit shaft friction. Test results were compared to current design methods. The k_f factor of the test results was dependent on the vertical effective stress. The traditional API method is normally considered to underestimate the shaft capacity of short piles in dense sand. However, compared to the more advanced CPT-based methods, the simplified ICP and offshore UWA, the test results showed better agreement with the predictions of the API method. A formulation of the k_f factor for the test results was suggested.

Due to the short length of the piles, each test was considered to provide a unique *t-z* curve for each effective stress level. When these curves were compared to current *t-z* curve formulations, the Zhang formulation, developed from tests on bored piles, gave a good prediction of the initial and post-peak parts of the *t-z* curves from the test results.

7. APPENDIX A

This appendix presents the four *t-z* curve formulations used in the analysis. The following symbols are used: *t* is the mobilized unit skin friction, *z* is the local axial pile deflection, t_{max} is the maximum unit skin friction with the corresponding axial pile deflection z_{tmax}, t_{res} is the residual unit skin friction over a post-peak displacement Δz_{res}, t_{post} is the residual unit skin friction at a post-peak displacement Δz, and η_{res} is a softening parameter.

7.1. API

The API (2011) provides the t-z curve formulation given in Table 5.

Table 5. *t-z* Curve Formulation in API (2011).

z/z_{max}	t/t_{max}
0.00	0.00
0.16	0.30
0.31	0.50
0.57	0.75
0.80	0.90
1.00	1.00
2.00	1.00
∞	1.00

7.2. Zhang Function

Zhang and Zhang (2013) propose the following formulations for *t-z* curves from tests on bored piles:

$$t = \frac{z(a+cz)}{(a+bz)^2} \tag{15}$$

$$t_{max} = \frac{1}{4(b-c)} \tag{16}$$

$$z_{t_{max}} = \frac{a}{b-2c} \tag{17}$$

$$a = (b-2c)z_{t_{max}} \tag{18}$$

$$b = \frac{1-\sqrt{1-\beta_s}}{2\beta_s}\frac{1}{t_{max}} \tag{19}$$

$$c = \frac{2-\beta_s-2\sqrt{1-\beta_s}}{4\beta_s}\frac{1}{t_{max}} \tag{20}$$

$$\beta_s = \frac{t_{res}}{t_{max}} \tag{21}$$

7.3. 80% Function

Fellenius (2013) gives the following formulation for the 80% function:

$$t = \frac{\sqrt{z}}{C_1 z + C_2} \tag{22}$$

$$C_1 = \frac{1}{2 t_{max} \sqrt{z_{t_{max}}}} \tag{23}$$

$$C_2 = \frac{\sqrt{z_{t_{max}}}}{2 t_{max}} \tag{24}$$

7.4. Parabolic Function

Randolph and Gourvenec (2011) suggest a parabolic function for t-z curves:

$$t_{ini} = t_{max} \left(2 \cdot \frac{z}{z_{t_{max}}} - \left(\frac{z}{z_{t_{max}}} \right)^2 \right) \tag{25}$$

$$t_{post} = t_{max} - 1.1 (t_{max} - t_{res}) \left(1 - \exp \left(-2.4 \left(\frac{\Delta z}{\Delta z_{res}} \right)^{\eta_{res}} \right) \right) \tag{26}$$

8. ACKNOWLEDGMENTS

9. REFERENCES

API (American Petroleum Institute) (2011). "Geotechnical and Foundation Design Considerations." *API RP 2GEO/ISO 19901-4*, 1st Edition, American Petroleum Institute.

Baeβler, M., Rücker, W., Cuéllar, P., Georgi, S. and Karbeliov, K. (2013), "Large-Scale Testing Facility for Cyclic Axially Loaded Piles," *Steel Construction*, 6(3), 200–206.

Baldi, G., Belotti, R., Ghionna, V., Jamiolkowski, M. and Pascalini, E. (1986), "Interpretation of CPTs and CPTUs; 2nd part; drained penetration of sands." *Proc., 4th Int. Geotechnical Seminar*, 143–156.

Boulon, M. and Foray, P. (1986). "Physical and numerical simulation of lateral shaft friction along offshore piles in sand." *Proc., 3rd Int. Conf. on Numerical Methods in Offshore Piling*, Institut Français du Pétrole, Laboratoire Central des Ponts et Chaussées, 127–147.

Boulon M. (1989). "Basic features of soil structure interface behaviour." *Computers and Geotech.*, 7, 115–131.

Chan, S.-F. and Hanna, T.H. (1980), "Repeated Loading on Single Piles in Sand." *J. Geotech. Eng. Div.*, 106(2), 171–188.

Clausen, C.J.F., Aas, P.M., and Karlsrud, K. (2005). "Bearing capacity of driven piles in sand, the NGI approach." *Proc., Front. in Offshore Geotechnics (ISFOG 2005)*, S.

Gourvenec and M. Cassidy, eds., Taylor & Francis Group, London, UK, 677–681.

DNV (Det norske Veritas). (2010). "Design of offshore structures." *DNV-OS-J101*, Det norske Veritas Classification A/S.

Fellenius, B.H. (2013), Discussion on Zhang, Q.Q. and Zhang, Z.M. (2012). "A simplified non-linear approach for single pile settlement analysis." *Can. Geotech. J.*, 50(6), 685–687.

Foray, P. (1991). "Scale and boundary effects on calibration chamber pile tests." *Proc., 1st Int. Symp. on Calibration Chamber Testing/ISOCCT1*, Elsevier, 147–160.

Gaydadzhiev, D., Puscasu, I., Vaitkunaite, E. and Ibsen, L.B. (2015). "Investigation of dense sand properties in shallow depths using CPT and DMT." *Proc., 3rd Int. Conf. on the Flat Dilatometer*, International Society for Soil Mechanics and Geotechnical Engineering, 223–230.

Ghionna, V.N. and Jamiolkowski, M. (1991). "A critical appraisal of calibration chamber testing of sands." *Proc., 1st Int. Symp. on Calibration Chamber Testing/ISOCCT1*, Elsevier, 13–39.

Hammad, W. (1991). *Modélisation non linéaire et étude expérimentale des bandes de cisaillement dans le sable*, Thèse de doctorat, Université Joseph Fourier, Grenoble, France.

Hedegaard, J. and Borup, M. (1993). *Klassifikationsforsøg med Baskarp-sand No. 15*. Aalborg Universitetscenter.

Ho, T.Y.K., Jardine, R.J. and Anh-Minh, N. (2011). "Large-displacement interface shear between steel and granular media." *Géotechnique*, 61(3), 221–234.

Huang A.-B. and Hsu, H.-H. (2005). "Cone penetration tests under simulated field conditions." *Géotechnique*, 55(5), 345–354.

Ibsen, L.B., Hanson, M., Hjort, T. and Thaarup, M. (2009). "MC–Parameter Calibration of Baskarp Sand No. 15." *DCE Technical Report No. 62*, Department of Civil Engineering, Aalborg University, Denmark.

Jardine, R.J., Bitang, Z., Foray, P. and Dalton, C.P. (2009). "Experimental Arrangements for Investigation of Soil Stresses Developed around a Displacement Piles." *Soils and Foundations*, 49(5), 661–673.

Jardine, R.J., Chow, F.C., Overy, R.F. and Standing, J.R. (2005). *ICP design methods for driven piles in sands and clays,* Thomas Telford, London.

Jardine, R.J., Lehane, B.M. and Everton, S.J. (1992). "Friction coefficients for piles in sands and silts." *Proc., Int. Conf. on Offshore Site Investigation and Foundation Behaviour*, Society for Underwater Technology, Springer Netherlands, 661–677.

Jardine, R.J. and Standing, J.R. (2012). "Field Axial Cyclic Loading Experiments on Piles Driven in Sand." *Soils and Foundations*, 52(4), 723–736.

Lehane, B.M., Jardine, R.J., Bond, A.J. and Frank, R. (1993). "Mechanisms of shaft friction on sand from instrumented pile tests." *J. Geotech. Eng.*, 119(1), 19–35.

Lehane, B.M., Schneider, J.A. and Xu, X. (2005a). *A Review of Design Methods for Offshore Driven Piles in Siliceous Sand,* The University of Western Australia.

Lehane, B.M., Schneider, J.A. and Xu, X. (2005b), "The UWA-05 method for prediction of axial capacity of driven piles in sand." *Proc., Front. in Offshore Geotechnics (ISFOG 2005)*, S. Gourvenec and M. Cassidy, eds., Taylor & Francis Group, London, UK, 661–667.

Le Kouby, A., Canou, C. and Dupla, J.C. (2004), "Behaviour of Model Piles subjected to Cyclic Axial Loading." *Proc., Int. Conf. Cyclic Behaviour of Soils and Liquefaction Phenomena*, Taylor & Francis Group, London, UK, 159–166.

Le Kouby, A., Dubla, J.C., Canou, J. and Francis, R. (2013), "Pile response in sand: experimental development and study." *Int. J. Phys. Model. Geotech.*, 13(4), 122–137.

Mortara, G., Mangiola, A. and Ghionna, V.N. (2007). "Cyclic shear stress degradation and post-cyclic behaviour from sand-steel interface direct shear tests." *Can. Geotech. J.*, 44, 739–752.

Prai-ai, S. (2013). *Behaviour of soil-structure interfaces subjected to a large number of cycles. Application to piles,* PhD thesis, University of Grenoble.

Randolph, M. and Gourvenec, S. (2011). *Offshore Geotechnical Engineering*: Piled foundations, 145–235, CRC Press, Taylor and Francis Group, London.

Salgado, R., Mitchell, J.K. and Jamiolkowski, M. (1998). "Calibration Chamber Size Effects on Penetration Resistance in Sand." *J. Geotech. Geoenviron. Eng.*, 124(9), 878–887.

Schnaid, F. and Houlsby, G.T. (1991). "An assessment of chamber size effects on the calibration of in situ tests in sand." *Géotechnique*, 41(3), 437–445.

Uesugi M. and Kishida, H. (1986). "Influential factors of friction between steel and dry sand", *Soils and foundations*, 26(2), 33–46.

Zhang, Q.Q. and Zhang, Z.M. (2012). "A simplified non-linear approach for single pile settlement analysis." *Can. Geotech. J.*, 49(11), 1256–1266.